RADIATION RESEARCH **173**, 719–728 (2010)
0033-7587/10 $15.00

DOI: 10.1667/RR1984.1

Gold Nanoparticles as Radiation Sensitizers in Cancer Therapy

Devika B. Chithrani,[a,b,1] Salomeh Jelveh,[c] Farid Jalali,[b] Monique van Prooijen,[b] Christine Allen,[d] Robert G. Bristow,[c,e] Richard P. Hill[c,e] and David A. Jaffray[a,b,e]

[a] *STTARR Innovation Centre, University Health Network, Toronto, Ontario, Canada;* [b] *Radiation Medicine Program, Princess Margaret Hospital, University Health Network, Toronto, Ontario, Canada;* [c] *Ontario Cancer Institute, University Health Network, Toronto, Ontario, Canada;* [d] *Leslie Dan Faculty of Pharmacy, University of Toronto, Toronto, Ontario, Canada; and* [e] *Departments of Radiation Oncology and Medical Biophysics, University of Toronto, Toronto, Canada*

Chithrani, B. D., Jelveh, S., Jalali, F., Van Prooijen, M., Allen, C., Bristow, R. G., Hill, R. P. and Jaffray, D. A. Gold Nanoparticles as Radiation Sensitizers in Cancer Therapy. *Radiat. Res.* 173, 719–728 (2010).

Among other nanoparticle systems, gold nanoparticles have been explored as radiosensitizers. While most of the research in this area has focused on either gold nanoparticles with diameters of less than 2 nm or particles with micrometer dimensions, it has been shown that nanoparticles 50 nm in diameter have the highest cellular uptake. We present the results of *in vitro* studies that focus on the radiosensitization properties of nanoparticles in the size range from 14–74 nm. Radiosensitization was dependent on the number of gold nanoparticles internalized within the cells. Gold nanoparticles 50-nm in diameter showed the highest radiosensitization enhancement factor (REF) (1.43 at 220 kVp) compared to gold nanoparticles of 14 and 74 nm (1.20 and 1.26, respectively). Using 50-nm gold nanoparticles, the REF for lower- (105 kVp) and higher- (6 MVp) energy photons was 1.66 and 1.17, respectively. DNA double-strand breaks were quantified using radiation-induced foci of γ-H2AX and 53BP1, and a modest increase in the number of foci per nucleus was observed in irradiated cell populations with internalized gold nanoparticles. The outcome of this research will enable the optimization of gold nanoparticle-based sensitizers for use in therapy.

INTRODUCTION

Each year 10.9 million people worldwide are diagnosed with cancer, and there are 6.7 million deaths from the disease (*1*). It is estimated that there are 24.6 million people alive who have received a diagnosis of cancer in the last 5 years. Approximately half of the people who develop cancer each year receive radiation therapy as a component of their treatment. Delivering a curative dose of radiation to tumor tissues while sparing normal tissues is still a great challenge in radiation therapy. The concept of using high-Z materials to increase the dose given to a tumor during radiation therapy was advanced over 20 years ago when iodine was shown by Matsudaira *et al.* to sensitize cultured cells (*2*). Santos Mello *et al.* found that direct intratumoral injection of iodine with radiation suppressed the growth of 80% of tumors in mice (*3*). Norman *et al.* modified a CT scanner to deliver tomographic orthovoltage (140 kVp) X rays to spontaneous canine brain tumors after intravenous injection with iodine contrast medium, which resulted in 53% longer survival (*4, 5*). Nath *et al.* demonstrated enhancement of radiosensitivity by a factor of three by incorporating iodine into cellular DNA with iododeoxyuridine *in vitro* (*6*).

However, the use of gold as a radiosensitizer seems more promising than the earlier attempts using iodine since gold has a higher Z number than iodine and has greater biocompatibility (*2–4, 7–9*). Investigations of the *in vitro* toxicity of gold nanoparticles have shown cytotoxicity for smaller gold nanoparticles (1–2 nm) but not for the larger gold nanoparticles (*9, 10*). Both theoretical and experimental studies have demonstrated greater dose enhancement effects for irradiations close to the surface of a thin metallic gold foil (*11, 12*). Herold *et al.* demonstrated dose enhancement for cells suspended in 1% gold particle solutions (dimensions of particles were 1.5–3.0 μm) as well as for tumors injected with gold microspheres (*13*). As shown by Herold *et al.*, it would be very difficult to deliver high-Z materials uniformly throughout the tumor as microspheres, primarily because of the size of the particles. Hainfeld and Rashman *et al.* used smaller gold particles with dimensions of 1.9 nm to overcome these difficulties (*14–16*). The concentration of the gold at the tumor site was 0.7%. The dose administered to achieve this level in tumors is too high for translation to humans. Nanoparticles with dimensions up to 100 nm can traverse the cell membrane and may accumulate preferentially in cancer cells (*17, 18*). Such nanoparticles (1–100 nm) are smaller than the typical cutoff size of the pores in tumor

[1] Address for correspondence: STTARR/Radiation Medicine Program, Princess Margaret Hospital, 7th Floor, 101, College Street, M5G 1L7, Toronto, ON, Canada; e-mail: devika.chithrani@rmp.uhn.on.ca.

vasculature (e.g., up to 400 nm) so they may access cells in tumors (*19*). Most research to date has used either gold nanoparticles of size 2–13 nm or larger particles with micrometer dimensions (*13, 20–23*). According to a recent theoretical study, gold nanoparticles of size between 2–10 nm or larger particles with micrometer dimensions would be expected to have a very low cell uptake (*24*). Consistent with this study, our recent *in vitro* work has confirmed that cellular uptake of nanoparticles is dependent on their size. Nanoparticles 50 nm in diameter showed the highest uptake into cells (*25–29*).

The goal of the present study was to optimize the uptake of gold nanoparticles within the cell and to investigate radiosensitization as a function of gold nanoparticle size and dose using therapeutic X rays with a range of different energies. The concentration of the gold nanoparticle solutions used in this study was 1×10^{-3}% (~1 n*M*), which is much lower than the concentrations used previously *in vivo* (*13, 14*). However, more recent studies are identifying the potential for much lower concentrations *in vivo* (*21, 22*). The mechanism of action for this effect is likely dependent on intracellular and potentially nuclear localization (*30*). We believe that cellular uptake producing much higher intracellular concentrations is a prerequisite for radiosensitization (*25–27*). In this study, we evaluated the radiobiological response for gold nanoparticles with well-characterized intracellular uptake characteristics. In addition, we quantified the enhancement of radiation-induced double-strand breaks (DSBs) in cells containing internalized gold nanoparticles using γ-H2AX and 53BP1 focus assays. We present evidence of the enhancement of radiation sensitization in cells with internalized gold nanoparticles at megavoltage energies used in conventional radiation practice (6 MVp) and at concentrations feasible for use in humans (*30*). New developments in nanotechnology offer great potential for improvements in the care of cancer patients (*31–33*).

MATERIALS AND METHODS

Synthesis of Gold Nanoparticles

Gold nanoparticles of different sizes were synthesized using the citrate reduction method (*34*). Different sizes of nanoparticles were prepared by changing the ratio between the gold salt and the reducing agent. First, 300 μl of 1% $HAuCl_4.3H_2O$ (Sigma-Aldrich) was added to 30 ml of double-distilled water and heated on a hot plate while stirring. Once it reached the boiling point, 600, 300 or 260 μl of 1% anhydrous citric acid (Sigma-Aldrich) was added to form nanoparticles 14, 50 or 74 nm in diameter, respectively. After the color of the solution changed from dark blue to red, the solution was left to boil for another 5 min while stirring. Finally, the gold nanoparticle solution was brought to room temperature while stirring.

Cell Culture Studies

HeLa cells were cultured in Dulbecco's modified Eagle's medium (DMEM) supplemented with 10% FBS. Cells were incubated at 37°C in a humidified incubator with 95% air/5% CO_2. For cellular uptake studies, the cells were grown in petri dishes (Fisherbrand, 60 × 15 mm) until they reached 80% confluence and incubated with fresh medium for 3 h before nanoparticles were introduced. The extra citrate in the gold nanoparticle solution was removed by centrifugation before the gold nanoparticles were introduced into the medium containing serum proteins (7×10^9 nanoparticles/ml). Uptake of gold nanoparticles is believed to be mediated by adsorption of serum proteins onto the surface of the nanoparticles (*25, 35, 36*). TEM images of the gold nanoparticles incubated in medium with serum proteins showed no sign of aggregation after 8 h of incubation. This was further verified by characterization of gold nanoparticles used in the experiments by DLS (dynamic light scattering) and zeta potential measurements before and after the incubation with the medium containing serum proteins; and the data are shown in Section S1 of the Supplementary Information. After 8 h of incubation with gold nanoparticles, the cells were washed three times with PBS and trypsinized for quantification of the number of gold nanoparticles present per cell. Cells were counted and then treated with HNO_3 at 200°C in an oil bath for ICP-AES analysis (see Supplementary Information, Sections S2 and S3).

TEM Analysis of Cells with Internalized Nanoparticles

Cells incubated with nanoparticles as above were washed three times with PBS and fixed (2.5% paraformaldehyde, 0.5% glutaraldehyde) for 8 h. The cells were then postfixed in 1% osmium tetroxide for 2 h, washed and dehydrated in graded concentrations of ethanol (25%, 50%, 70% and 100%) and propylene oxide. Cell samples were then embedded in Epon (Polysciences Inc.) and sectioned. Thin sections of 60–70 nm were collected on copper grids and stained with a 1:1 mixture of methanol and lead citrate. The grids were visualized using an H7000 TEM (Hitachi Corp., Japan).

Radiation Sources

The two lowest energies were obtained from a Gulmay D3225 orthovoltage unit at dose rates of 4.7 Gy/min at 105 kVp and 2.3 Gy/min at 220 kVp. The 660 keV energy came from a ^{137}Cs irradiator unit at a dose rate of 88 cGy/min. An Elekta Synergy was used for irradiations with a 6 MV beam at a dose rate of 600 MU/min, where 1 MU is equivalent to 1 cGy at a depth of 1.5 cm in a 10 × 10-cm^2 field.

Dose Calculations for Cell Irradiations

Individual dosimetry calculations were performed for the 105 kVp, 220 kVp and 6 MVp irradiations using clinical calculation methods and were confirmed using Gafchromic film (EBT) in contact with base of the petri dish. For dosimetry, the medium in the petri dish was considered as water. Reference dosimetry for the orthovoltage (dose to muscle) and megavoltage (dose to water) beams is performed using TG-61 and TG-51 protocols, respectively, and these units are under annual assessment through internal and external dosimetry services. Irradiations with ^{137}Cs were performed in a research irradiator with dosimetry confirmed using Gafchromic film (10%) (see Supplementary Information, Section S4).

Clonogenic Assay

HeLa cells were grown in DMEM/h21 medium at 37°C in a humidified incubator with 95% air/5% CO_2. The cells were first seeded at 10^6 cells in four tissue culture dishes and incubated for 24 h. To investigate the dependence of nanoparticle size on radiation response, medium containing gold nanoparticles of 14, 50 or 74 nm in diameter was added separately to three different flasks (concentration 7×10^9 nanoparticles/ml) and incubated for another 24 h. The flasks were trypsinized, and different dilutions were made from the cells incubated with and without gold nanoparticles to produce an

expected (based on preliminary studies) average of 50 colonies in 10-cm dishes after 2, 4, 6 and 8 Gy. Gold nanoparticles of the corresponding size were then added to each dish containing cells already incubated with gold nanoparticles (concentration 7×10^9 nanoparticles/ml) to maintain the same concentration of gold nanoparticles in the medium during irradiation. The cells were then incubated for 3 h before irradiation and were kept on ice as soon as they were removed from the incubator for irradiation. After irradiation, cells were incubated for 2 weeks to form colonies. Methylene blue (0.1%) was used for staining the colonies. The colonies containing >50 cells were counted for calculating the surviving fractions. The plating efficiency of the cells was determined by counting the number of colonies at 0 Gy.

γ-H2AX Indirect Immunofluorescence Assay

HeLa cells were seeded into 6-cm dishes containing 18 × 18-mm cover slips. Once the cells adhered, gold nanoparticles were introduced into one set of dishes, leaving the other set of dishes as reference cells. Cells were incubated with gold nanoparticles for 24 h and subsequently irradiated with 4 Gy of 220 kVp and 6 MVp X rays. After irradiation, cells were returned to a 95% air/5% CO_2 37°C incubator and subsequently removed at the indicated times for fixation and analysis by indirect immunofluorescence. Cells were fixed with freshly prepared 2% paraformaldehyde (pH 8.2)-0.2% Triton X-100 for 20 min. Cover slips were washed three times with PBS, and the cells were permeabilized with 0.5% Nonidet P40 for 20 min and washed again with PBS. The cells were then blocked with 2% BSA-1% normal donkey serum for 1 h and then incubated with the appropriate antibodies diluted in 3% BSA overnight at 4°C. The following antibodies were used for these *in vitro* studies: γ-H2AX (mouse monoclonal, JBW301, Upstate) and 53BP1 (rabbit polyclonal (aa1308-1824), Alexis). After primary antibody incubation, the cover slips were washed three times with 0.175% Tween 20-0.5% BSA-PBS and incubated with donkey anti-mouse Alexa 488 (Invitrogen) and donkey anti-rabbit Alexa 555 (Invitrogen) secondary antibodies for 45 min at room temperature in the dark. The cover slips were washed again with 0.175% Tween 20-0.5% BSA-PBS and the cell nuclei were stained with 0.2 μg ml^{-1} 4′,6-diamidino-2-phenylindole (DAPI) for 10 min followed by three washes with PBS. The cover slips were mounted onto 1-mm glass microscope slides with Vectashield anti-fade (Vector Laboratories, Burlingame, CA).

The cells were imaged using an Olympus IX81 inverted microscope controlled using In Vivo software (Media Cybernetics, Bethesda, MD). Three-dimensional data sets were obtained by acquiring 75 optical sections per field of view. Deconvolved images were analyzed using Image Pro Analyzer (Media Cybernetics) without further processing. Briefly, deconvolved image sets were maximum intensity projected and DAPI, Alexa 488 and Cy3 channels were separated. Only nonoverlapping DAPI-stained nuclei were used to generate outlines and masks.

RESULTS

Dependence of Cellular Uptake on the Size of the Gold Nanoparticles

Figure 1 illustrates the dependence of cellular uptake on the size of the gold nanoparticles as determined by transmission electron microscopy (TEM) (Fig. 1A) and UV-visible spectroscopy (Fig. 1B, left panel). The average diameters of the gold nanoparticles were 14, 50 and 74 nm with peak plasmon absorption wavelengths of 517, 534 and 550 nm, respectively (see Supplementary Information, Section S5). As shown on the right panel of Fig. 1B, nanoparticles of diameter 50 nm showed the highest cellular uptake. TEM images of fixed cells with internalized gold nanoparticles are shown in the panel of Fig. 1C; the gold nanoparticles are localized in small vesicles of size range ~300–500 nm.

Variation in Radiation Sensitization as a Function of Size of the Gold Nanoparticles

Figure 2 shows the variation in radiosensitization as a function of the size and concentration of the nanoparticles internalized within the cells. The left panel of Fig. 2A shows the survival curves for HeLa cells irradiated with 220 kVp X rays in the absence and presence of different-sized gold nanoparticles within the cells. The data were fitted with a linear-quadratic (LQ) model [$SF = \exp(-\alpha D - \beta D^2)$] and are shown as solid lines along with the data points. Values corresponding to the parameters α and β and the goodness of fit, χ^2, are listed in the Supplementary Information, Section S6. The radiation sensitization enhancement factor (REF) in the presence of gold nanoparticles of different sizes was calculated as the ratio of dose without gold nanoparticles/dose with gold nanoparticles at 10% survival. The right panel of Fig. 2A further summarizes the differences in the sensitization properties of the different-sized gold nanoparticles; cells that internalized 50-nm gold nanoparticles showed the greatest sensitization. As illustrated in the left panel of Fig. 2B, this effect appears to be related to the higher number of nanoparticles present in the cells since the total amount of gold in the cells increased with the size of the nanoparticles despite the lower uptake of the 74-nm nanoparticles. This was verified by evaluating the variation in radiation response as a function of the number of internalized gold nanoparticles by changing the concentration of gold nanoparticles in the medium (Fig. 2B, right panel). Fifty-nanometer gold nanoparticles were used for this study.

Dependence of Sensitization on the Energy of the Radiation Source

To investigate the dependence of radiation sensitization on the energies of the X or γ rays, cells were treated with 50-nm gold nanoparticles and survival curves were generated for four different energies [105 kVp, 220 kVp, ^{137}Cs (660 keV) and 6 MVp) (Fig. 3)]. Greater radiation sensitization was seen for cells irradiated with the lower-energy radiation beams (see Supplementary Information, Section S5). The fitting parameters for the LQ fits to the survival curves and the REF values in the presence of gold nanoparticles at 10% survival are listed in Table 1.

Assessment of the Enhancement of DNA DSBs in Cells with Internalized Gold Nanoparticles

Figures 4 and 5 show DNA DSBs in cells irradiated with 4 Gy of 220 kVp and 6 MVp X rays, respectively.

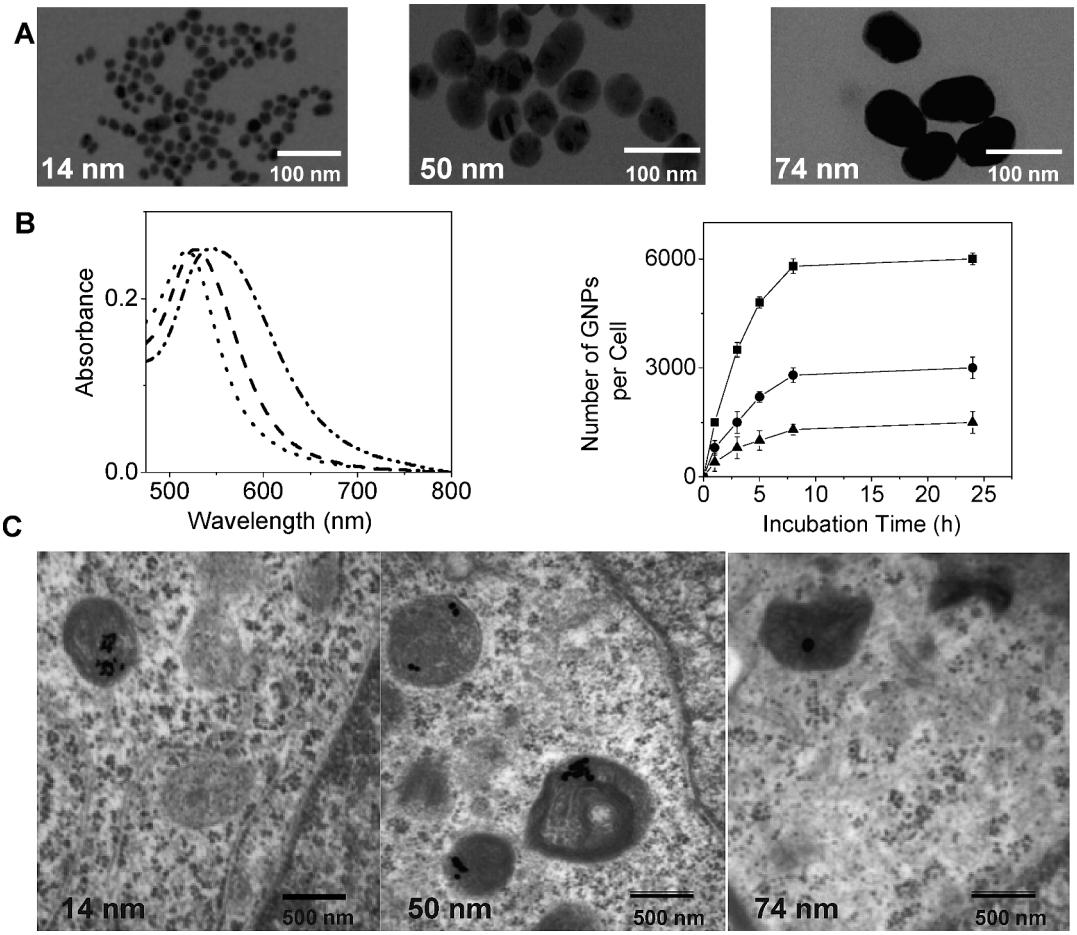

FIG. 1. Cell uptake studies. Panel A: TEM image of gold nanoparticles of 14, 50 and 74 nm in diameter. Panel B, left: UV-visible spectra of gold nanoparticles 14 (dotted line), 50 (dashed line) and 74 (dash dot line) nm in diameter. Panel B, right: Cellular uptake of gold nanoparticles 14 (▲), 50 (■) and 74 (●) nm in diameter. Points are means ± SD for three experiments. Panel C: TEM images of cells with internalized gold nanoparticles 14 (left), 50 (middle) and 74 (right) nm in diameter.

The experimental setups for the irradiations are shown in the left panel of Figs. 4A and 5A. To quantify the DSBs, a minimum of 50 nuclei from each sample were assayed using image intensity-based thresholding and segmentation. Two proteins, γ-H2AX and 53BP1, that are present at the sites of DNA DSBs were probed using wide-field imaging. The results are shown in the right panel of Figs. 4A and 5A. The top and bottom panels in Figs. 4B and 5B show images corresponding to several nuclei of the reference cells (without nanoparticles) and cells with nanoparticles, respectively. These images correspond to several nuclei of cells that were irradiated and fixed 4 h later. The three columns in Fig. 4B and Fig. 5B represent images of the same field of view for γ-H2AX, 53BP1 and composite, respectively.

DISCUSSION

Most of the recent research on radiosensitization by gold particles has focused on either very small particles (1.9 and 13 nm) or much larger particles (1.5–3.0 μm) (*13, 14, 22, 23*). According to Gao *et al.*, particles with these diameters would have very low uptake into cells; they predicted that the optimum diameter for uptake would be about 50 nm (*24*). Since it is anticipated that radiosensitization effects can be optimized by increasing the uptake of gold nanoparticles into cells, our first goal was to optimize the uptake of gold nanoparticles at the cellular level by tailoring the size of the gold nanoparticles for this optimum region. The results in Fig. 1 show that cellular uptake of gold nanoparticles was dependent on the size and are in agreement with previous reports (*25–29*). Gold nanoparticles 50 nm in diameter had the highest uptake. This optimal size for the endocytosis process is a result of competition between the thermodynamic driving force for cell uptake and receptor diffusion kinetics. For nanoparticles smaller than the optimal size, the increased elastic energy associated with bending of the membrane results in decreased driving force for membrane wrapping. When the particle size is smaller, membrane wrapping causes an increase in free energy and cannot proceed. For particles larger than the

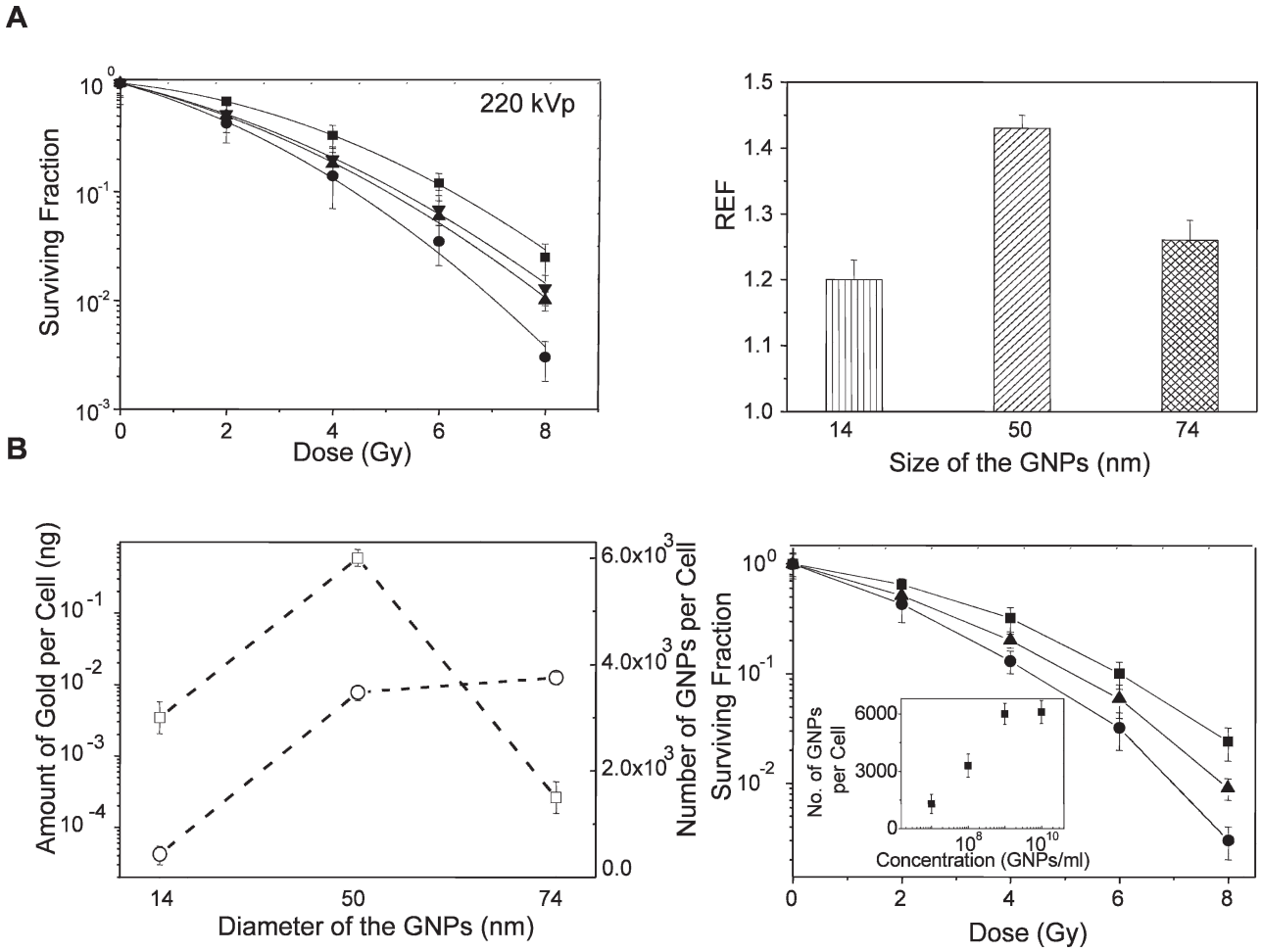

FIG. 2. Effect of size of the gold nanoparticles on radiation sensitization. Panel A, left: Variation in the surviving fraction of cells with no internalized gold nanoparticles (■) and cells with internalized gold nanoparticles 14 (▼), 50 (●) and 74 (▲) nm in diameter. Panel A, right: Radiation sensitization enhancement factors (REFs) for different-sized nanoparticles. Panel B, left: Radiation sensitization as a function of number of gold nanoparticles internalized (□) and total mass of the gold internalized per cell (○) for different-sized gold nanoparticles. Panel B, right: Surviving fraction as a function of concentration of gold nanoparticles in the medium [1×10^9 gold nanoparticles/ml (●), 1×10^8 gold nanoparticles/ml (▲), 1×10^7 gold nanoparticles/ml (■)]. Inset shows the uptake of gold nanoparticles as a function of concentration of gold nanoparticles in the medium. Points are means ± SD for three experiments. GNPs, gold nanoparticles.

optimum size, diffusion of receptors over a longer distance, and thus a longer wrapping time, is required. The TEM images in Fig. 1C show gold nanoparticles of different sizes internalized within cells. These nanoparticles were localized in small vesicles of size ~500 nm within the cell cytoplasm. However, nanoparticles were not localized in the nucleus, only accumulating close to the nuclear membrane with time.

Our next goal was to study radiation sensitization by gold nanoparticles bracketing the diameter for optimum uptake (14–74 nm). Previous studies showed radiosensitization of DNA by different size gold nanoparticles; to our knowledge, this is the first report of radiation sensitization by different-sized gold nanoparticles internalized in tumor cells (*37, 38*). Lower-energy X rays (220 kVp) were used to study radiation sensitization as a function of nanoparticle diameter. As shown in Fig. 2A, cells that had internalized 50-nm gold nanoparticles showed greater radiosensitization than cells that internalized nanoparticles 14 and 74 nm in diameter even though the extracellular concentration of gold nanoparticles was the same for each particle size. This is likely a result of higher concentration of gold nanoparticles in the cells incubated with gold nanoparticles 50 nm in diameter (Fig. 1B, right panel), since the total gold content in the cells increases with the size of the nanoparticles and is different for the 14-nm and 74-nm particles, which show similar levels of radiation sensitization (Fig. 2B, left panel). As illustrated in the right panel in Fig. 2B, the dependence of radiation sensitization on the number of internalized gold nanoparticles was verified by changing the number of internalized gold nanoparticles by varying the concentration of gold nanoparticles in the medium (Fig. 2B,

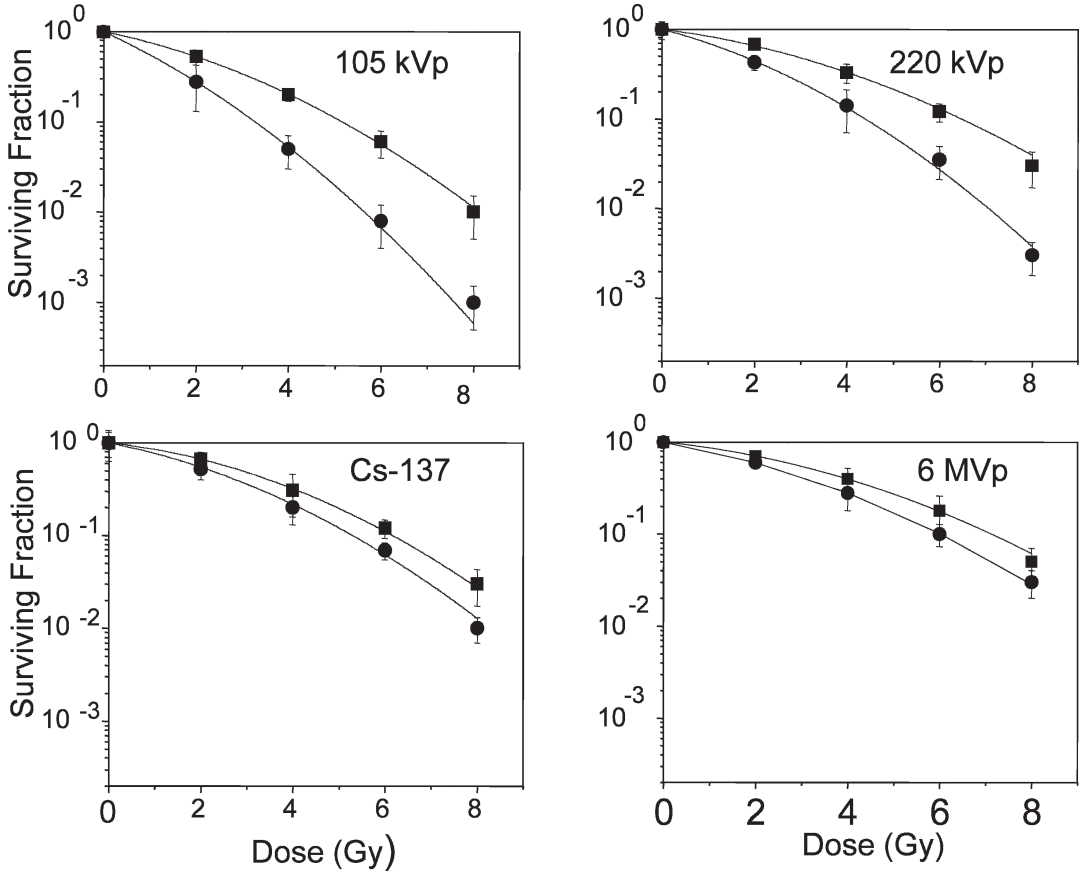

FIG. 3. Energy-dependent radiation response. Cell survival curves for energies of 105 kVp, 200 kVp, 660 keV (^{137}Cs) and 6 MVp (● in each panel), (■) Cells with no internalized gold nanoparticles. Points are means ± SD for three experiments. The solid lines are the fit to the LQ model.

right panel). As shown in Fig. 2, the size and concentration of gold nanoparticles play an important role in radiosensitization.

Greater uptake of gold nanoparticles (Fig. 2) leads to higher concentrations gold nanoparticles within the cells, leading to enhanced radiosensitization (Fig. 1). Thus we believe that size and the concentration of the nanoparticles play important roles in designing radiation treatments involving gold nanoparticles. Furthermore, nanoparticles of this size can be passively targeted to tumors by exploitation of their ''leaky'' vasculature and poor lymphatic drainage, a phenomenon known as the enhanced permeation and retention effect (*20, 39*). These observations combined with our results should enable researchers to design gold nanoparticle-based sensitizers optimized for radiation sensitization *in vivo*.

The desire to use these sensitizers at megavoltage energies required investigation of the radiation sensitization properties of gold nanoparticles as a function of beam energy. For this study, 50-nm gold nanoparticles were chosen since they showed the greatest radiation sensitization at 220 kVp. For the first time, we found evidence of enhancement of radiation sensitization at clinically relevant X-ray energies (6 MVp) for cells with internalized gold nanoparticles. While we expect a decrease in radiation sensitization at higher energies

TABLE 1
Fitted Parameters of the LQ Model for Experimental Data Shown in Fig. 3

	105 kVp	220 kVp	^{137}Cs	6 MVp
$\alpha_{control}$	0.237 ± 0.005	0.150 ± 0.004	0.119 ± 0.013	0.110 ± 0.008
$\beta_{control}$	0.041 ± 0.002	0.041 ± 0.001	0.040 ± 0.003	0.029 ± 0.002
α_{gold}	0.528 ± 0.007	0.352 ± 0.005	0.259 ± 0.011	0.191 ± 0.002
β_{gold}	0.054 ± 0.003	0.041 ± 0.002	0.030 ± 0.003	0.031 ± 0.001
$\chi^2_{control}$	8×10^{-6}	1×10^{-5}	8×10^{-5}	6×10^{-5}
χ^2_{gold}	2×10^{-6}	4×10^{-6}	3×10^{-5}	1×10^{-6}
REF	1.66 ± 0.05	1.43 ± 0.02	1.18 ± 0.03	1.17 ± 0.02

Note. REFs were calculated as the ratio of doses without GNPs/dose with GNPs at 10% survival.

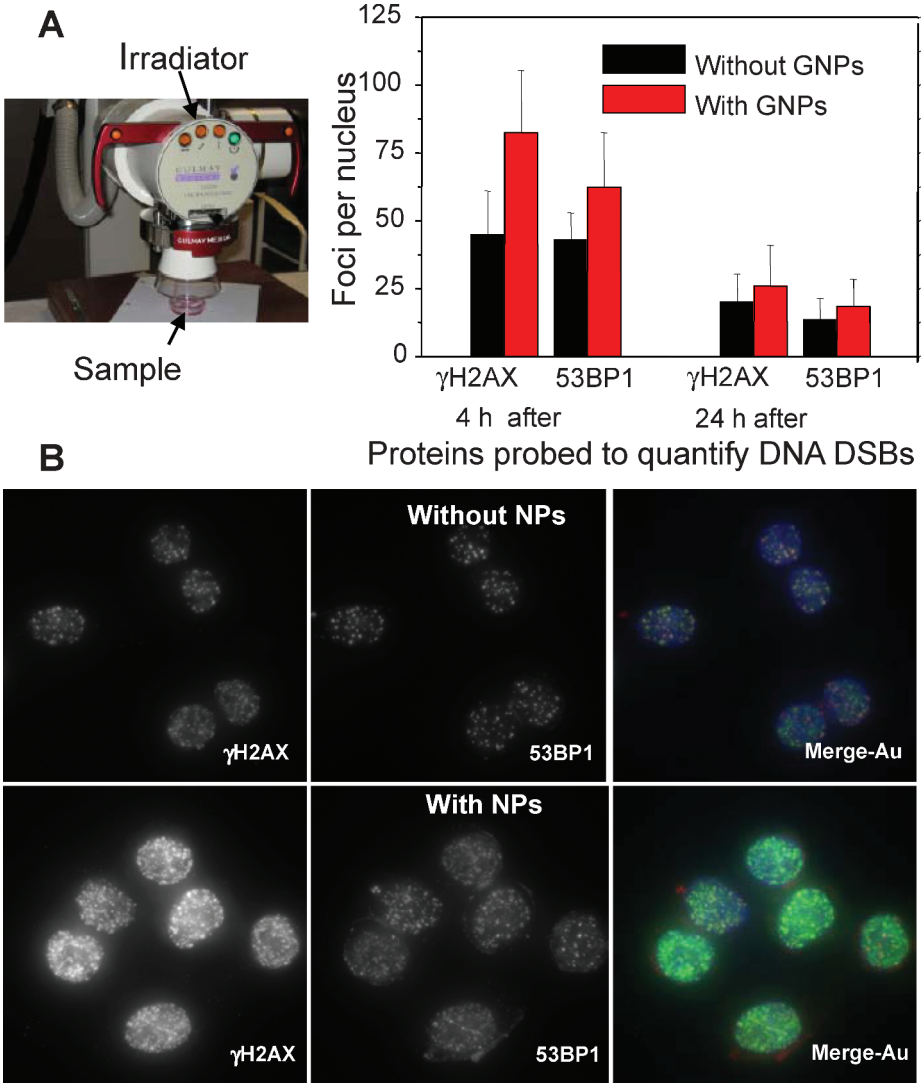

FIG. 4. Qualitative and quantitative analysis of DNA damage using lower-energy X-ray photons (220 kVp). Panel A, left: Setup used for the irradiations. Panel A, right: Quantification of γ-H2AX and 53BP1 radiation-induced foci after 4 Gy of 220 kVp X rays [cells pretreated with gold nanoparticles (red) and with no gold nanoparticle pretreatment (black)]. Panel B: Representative images of HeLa cells irradiated with 4 Gy and fixed for indirect immunofluorescence 4 h later. Top panels show cells with no gold nanoparticles and bottom panels show cells with gold nanoparticles. Points are means ± SD for three experiments.

(see Fig. 3), the measured effect exceeded the theoretically predicted dose enhancement (*40*). The experimental data in Fig. 3 were fitted with an LQ equation (*41*). The dose corresponding to 10% survival of HeLa cells was in agreement with that in previous reports (*42–45*). Table 1 summarizes the fit parameters (α and β) and the REF at 10% survival. The changes in sensitivity with gold nanoparticle are characterized by changes in the linear parameter (α) with no significant change in the quadratic parameter (β). This suggests that the effect is consistent with an increase in dose; however, the predicted increase in dose at MV energies is negligible (*40*). Considering the work of Zheng *et al.* (*30*), the enhancements due to gold nanoparticles would have two components, one related to an increase in cross section and the other related to the production of low-energy electrons. Detailed calculations of the dose delivered in the gold nanoparticle and control conditions would allow these two effects to be isolated. Such studies would allow the energy dependence of the low-energy electron component to be quantified.

Given the novelty of our results, we performed independent verification using quantified enhancement of DNA DSBs in cells 4 and 24 h after irradiation. Exposure to ionizing radiation results in the production of a variety of DNA lesions including single-strand breaks (SSBs), DSBs, DNA-base alterations, and DNA-DNA or DNA-protein crosslinks (*46*). DSBs are the most lethal, and in this study we examined the proteins γ-H2AX and 53BP1, which are associated with the sites

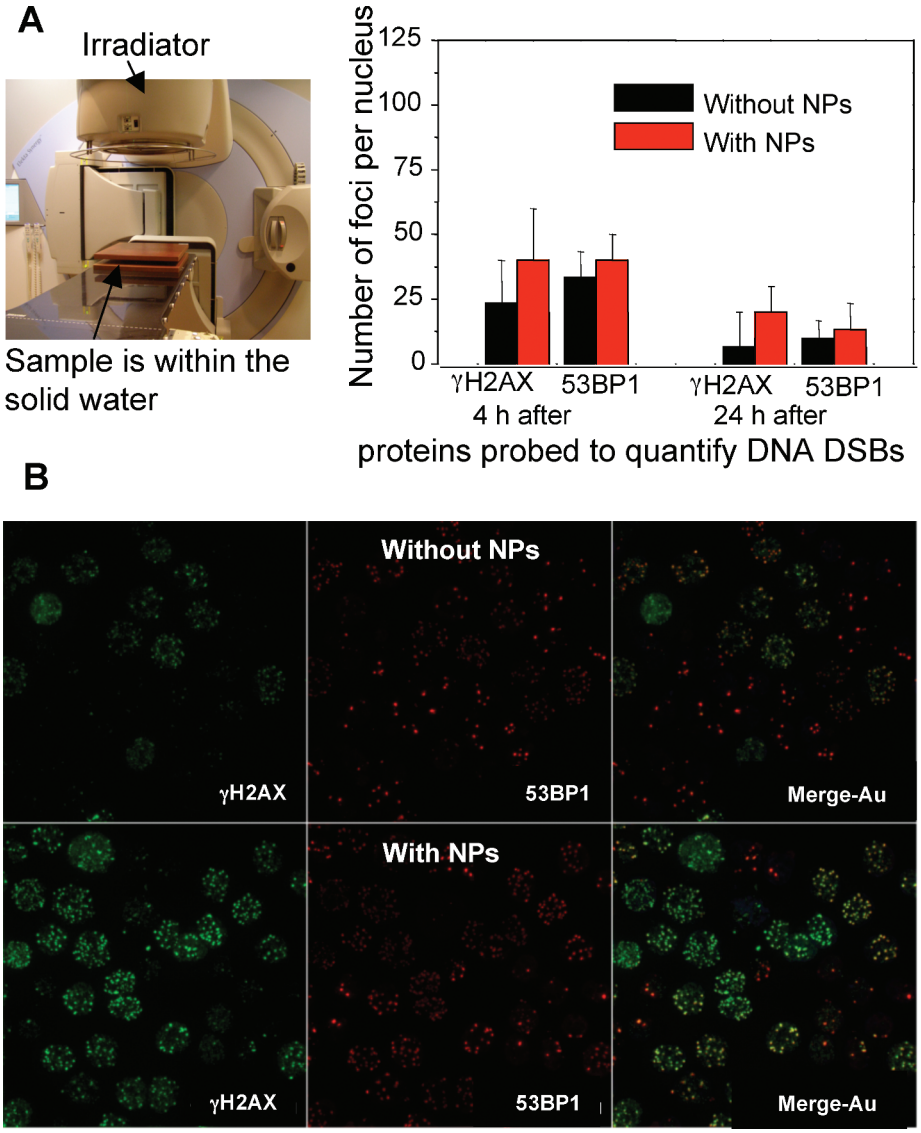

FIG. 5. Qualitative and quantitative analysis of DNA damage using 6 MVp X rays. Panel A, left: Setup used for the irradiations. Panel A, right: Quantification of γ-H2AX and 53BP1 radiation-induced foci after 4 Gy 6 MV photons [cells pretreated with gold nanoparticles (red) and with no gold nanoparticle pretreatment (black)]. Panel B: Representative images of HeLa cells irradiated with 4 Gy and fixed for indirect immunofluorescence 24 h later. Top panels show cells with no gold nanoparticles and bottom panels show cells with gold nanoparticles. Bars are means ± SD for three experiments. GNPs, gold nanoparticles.

of DSBs (*47–49*). Olive *et al.* have shown a direct correlation between γ-H2AX and clonogenic radiation cell survival *in vitro* (*49*). Figures 4 and 5 show the extent of DSBs for cells with internalized nanoparticles compared to cells with no gold nanoparticles irradiated with 220 kVp and 6 MV X rays, respectively. The quantification of DSBs using foci at 4 and 24 h provided a measure of the DSBs remaining with and without treatment. The use of both 53BP1 and γ-H2AX allowed for direct comparison and colocalization of these markers given that γ-H2AX (but not 53BP1) can be associated variably with apoptosis and chromatin compaction in early mitosis. These times were used by a number of investigators to look at residual breaks at early and late times after irradiation and to suggest that increased residual breaks can be one determinant of cell death in irradiated cells with nanoparticle or gold nanoparticle treatment. The increase in DSBs in cells with internalized gold nanoparticles is consistent with the clonogenic radiation cell survival *in vitro* for both lower and higher energies (see Fig. 3).

CONCLUSIONS

Over the past decade, there has been a great interest in using nanotechnology for cancer therapy. Our studies *in vitro* showed that radiosensitization was correlated with the average number of gold nanoparticles internalized

per cell. The survival of cells with internalized 50-nm gold nanoparticles was reduced for all irradiations due to the high cellular uptake of these gold nanoparticles compared to nanoparticles of other sizes. Radiation sensitization was observed for both lower- (100–220 kVp) and higher-energy (6 MVp) irradiations using a clonogenic assay and γ-H2AX assay of DSBs. This suggests that gold nanoparticles could be combined with radiation therapy for an increased therapeutic effect. Recent *in vivo* work has shown that nanoparticles of these dimensions can be effectively targeted to tumors by taking advantage of the enhanced permeation and retention effect (*39*), suggesting that the approach could allow an increase in the tumoricidal effects while moderating toxicity to normal tissues. McMahon *et al.* have pointed out the feasibility of dose localization through the combination of gold nanoparticles and targeted kilovoltage radiation to treat deep tumors, and the results are encouraging due to the large REF observed at kilovoltage radiation compared to megavoltage radiation (*50*). Zheng *et al.* recently demonstrated that the addition of gold nanoparticles to cisplatin and other platinum agents enhanced radiation damage (*51*). Therefore, gold nanoparticles in combination with radiations and chemotherapeutic drugs provide interesting avenues to further improve the treatment of cancer. Significant effort will be required to advance these observations through detailed studies of the mechanism of action and optimization of the effects. This will open up future applications of targeted radiosensitization in radiation therapy using physical processes.

SUPPLEMENTARY INFORMATION

Section S1: Characterization of uncoated and serum protein coated gold nanoparticles. Section S2: ICP-AES technique for characterization of concentration of gold nanoparticles. Section S3: Quantification of cellular uptake of gold nanoparticles using ICP-AES technique. Section S4: Dose calculations. Section S5: Statistical analysis. Section S6: Fitted parameters for the cell survival curves for HeLa cells irradiated with 220 kVp X rays in the absence and presence of different-sized gold nanoparticles within the cells. http://dx.doi.org/10.1667/RR1894.1.S1

ACKNOWLEDGEMENTS

The authors would like to thank Mr. Battista Calvieri, Mr. Steve Doyle, and Mr. Dan Mathers for their technical assistance in sample preparation and analysis. We would like to thank Prof. Leon Sanche from University of Sherbrooke for helpful discussions. The research work described in this manuscript was supported by Ontario Institute for Cancer Research, Canadian Institute for Health Research (CIHR), and the Fidani Radiation Physics Centre at Princess Margaret Hospital, Canada. It was also funded in part by the Ontario Ministry of Health and Long Term Care. The views expressed do not necessarily reflect those of the ONHLTC.

Received: June 17, 2009; accepted: December 14, 2009; published online: February 26, 2010

REFERENCES

1. B. W. Stewart and P. Kleihues, *World Cancer Report*. IARC Press, Lyon, 2003.
2. H. Matsudaira, A. M. Ueno and I. Furuno, Iodine contrast medium sensitizes cultured mammalian cells to X rays but not to γ rays. *Radiat. Res.* **84**, 144–148 (1980).
3. R. S. Mello, H. Callisen, J. Winter, A. R. Kagan and A. Norman, Radiation dose enhancement in tumors with iodine. *Med. Phys.* **10**, 75–78 (1983).
4. A. Norman, M. Ingram, R. G. Skillen, D. B Freshwater, K. S. Iwamoto and T. Solberg, X-ray phototherapy for canine brain masses. *Radiat. Oncol. Investig.* **5**, 8–14 (1997).
5. A. Norman, M. Ingram, S. T. Cochran, T. D Solberg and J. M. Ford, X-ray phototherapy for solid tumors. *Acad. Radiol.* **5**, S177–S179 (1998).
6. R. Nath, P. Bongiorni and S. Rockwell, Iododeoxyuridine radiosensitization by low- and high-energy photons for brachytherapy dose rates. *Radiat. Res.* **124**, 249–258 (1990).
7. E. E. Connor, J. Mwamuka, A. Gole, C. J. Murphy and M. D. Wyatt, Gold nanoparticles are taken up by human cells but do not cause acute cytotoxicity. *Small* **1**, 325–327 (2005).
8. R. Shukla, V. Bansal, M. Chaudhary, A. Basu, R. R. Bhonde and M. Sastry, Biocompatibility of gold nanoparticles and their endocytotic fate inside the cellular compartment: a microscopic overview. *Langmuir* **21**, 10644–10654 (2005).
9. N. Lewinski, V. Colvin and R. Drezek, Cytotoxicity of nanoparticles. *Small* **4**, 26–49 (2008).
10. Y. Pan, S. Neuss, A. Leifert, M. Fischler, F. Wen, U. Simon, G. Schmid, W. Brandau and W. Jahnen-Dechent, Size-dependent cytotoxicity of gold nanoparticles. *Small* **3**, 1941–1949 (2007).
11. D. F. Regulla, L. B. Hieber and M. Seidenbusch, Physical and biological interface dose effects in tissue due to X-ray-induced release of secondary radiation from metallic gold surfaces. *Radiat. Res.* **150**, 92–100 (1998).
12. D. L. Zellmer, J. D. Chapman, C. C. Stobbe, F. Xu and I. J. Das, Radiation fields backscattered from material interfaces: I. Biological effectiveness. *Radiat. Res.* **150**, 406–415 (1998).
13. D. M. Herold, I. J. Das, C. C. Stobbe, R. V. Iyer and J. D. Chapman, Gold microspheres: a selective technique for producing biologically effective dose enhancement. *Int. J. Radiat. Biol.* **76**, 1357–1364 (2000).
14. J. F Hainfeld, D. N. Slatkin and H. M. Smilowitz, The use of gold nanoparticles to enhance radiotherapy in mice. *Phys. Med. Biol.* **49**, N309–N315 (2004).
15. J. F. Hainfeld, C. J. Foley, S. C. Srivastava, L. F. Mausner, N. I. Feng, G. E. Meinken and Z. Steplewski, Radioactive gold cluster immunoconjugates: potential agents for cancer therapy. *Int. J. Radiat. Appl. Instrum. B* **17**, 287–294 (1990).
16. W. N. Rahman, N. Bishara, T. Ackerly, C. F. He, P. Jackson, C. Wong, R. Davidson and M. Geso, Enhancement of radiation effects by gold nanoparticles for superficial radiotherapy. *Nanomed. Nanotechnol. Biol. Med.* **5**, 136–142 (2009).
17. T. Niidome, K. Nakashima, H. Takahashi and Y. Niidome, Preparation of primary amine-modified gold nanoparticles and their transfection ability into cultivated cells. *Chem. Commun.* 1978–1979 (2004).
18. A. Anshup, J. S. Venkataraman, C. Subramaniam, R. R. Kumar, S. Priya, T. R. S. Kumar, R. V. Onkumar, A. John and T. Pradeep, Growth of gold nanoparticles in human cells. *Langmuir* **21**, 11562–11567 (2005).

19. S. Unezaki, K. Maruyama, J-I. Hosoda, I. Nagae, Y. Koyanagi and M. Nakata, Direct measurement of the extravasation of polyethyleneglycol-coated liposomes into solid tumor tissue by in vivo fluorescence microscopy. *Int. J. Pharm.* **144**, 11–17 (1996).
20. G. F. Paciotti, L. Myer, D. Weinreich, D. Goia, N. Pavel, R. E. McLaughlin and L. Tamarkin, Colloidal gold: a novel nanoparticle vector for tumor directed drug delivery. *Drug. Deliv.* **11**, 169–183 (2004).
21. X. Zhang, J. Z. Xing, J. Chen, L. Ko, J. Amanie, S. Gulavita, N. Pervez, D. Yee, R. Moore and W. Roa, Enhanced radiation sensitivity in prostate cancer by gold-nanoparticles. *Clin. Invest. Med.* **31**, E160–E167 (2008).
22. M. Y. Chang, A. L. Shiau, Y. H. Chen, C. J. Chang, H. H. Chen and C. L. Wu, Increased apoptotic potential and dose-enhancing effect of gold nanoparticles in combination with single-dose clinical electron beams on tumor-bearing mice. *Cancer Sci.* **99**, 1479–1484 (2008).
23. J. F. Hainfeld, F. A. Dilmanian, D. N. Slatkin and H. M. Smilowitz, Radiotherapy enhancement with gold nanoparticles. *J. Pharm. Pharmacol.* **60**, 977–985 (2008).
24. H. Gao, W. Shi and L. B. Freund, Mechanics of receptor-mediated endocytosis. *Proc. Natl. Acad. Sci. USA* **102**, 9469–9474 (2005).
25. B. D. Chithrani, A. A. Ghazani and W. C. Chan, Determining the size and shape dependence of gold nanoparticle uptake into mammalian cells. *Nano. Lett.* **6**, 662–668 (2006).
26. B. D. Chithrani and W. C. Chan, Elucidating the mechanism of cellular uptake and removal of protein-coated gold nanoparticles of different sizes and shapes. *Nano. Lett.* **7**, 1542–1550 (2007).
27. B. D. Chithrani, J. Stewart, C. Allen and D. A. Jaffray, Intracellular uptake, transport, and processing of nanostructures in cancer cells. *Nanomed. Nanotechnol. Biol. Med.* **5**, 118–127 (2009).
28. T. Nakai, T. Kanamori, S. Sando and Y. Aoyama, Remarkably size-regulated cell invasion by artificial viruses. Saccharide-dependent self-aggregation of glycoviruses and its consequences in glycoviral gene delivery. *J. Am. Chem. Soc.* **125**, 8465–8475 (2003).
29. F. Osaki, T. Kanamori, S. Sando, T. Sera and Y. Aoyama, A quantum dot conjugated sugar ball and its cellular uptake. On the size effects of endocytosis in the subviral region. *J. Am. Chem. Soc.* **126**, 6520–6521 (2004).
30. Y. Zheng, D. J. Hunting, P. Ayotte and L. Sanche, Radiosensitization of DNA by gold nanoparticles irradiated with high-energy electrons. *Radiat. Res.* **169**, 19–27 (2008).
31. A. G. Cuenca, H. Jiang, S. N. Hochwald, M. Delano, W. G. Cance and S. R. Grobmyer, Emerging implications of nanotechnology on cancer diagnostics and therapeutics. *Cancer* **107**, 459–466 (2006).
32. M. Ferrari, Cancer nanotechnology: opportunities and challenges. *Nat. Rev. Cancer* **5**, 161–171 (2005).
33. D. Peer, J. M. Karp, S. Hong, O. C. Farokhzad, R. Margalit and R. Langer, Nanocarriers as an emerging platform for cancer therapy. *Nat. Nanotechnol.* **2**, 751–760 (2007).
34. G. Frens, Controlled nucleation for the regulation of the particle size in monodisperse gold suspensions. *Nature (Lond.)* **241**, 20–22 (1973).
35. J. A. Khan, B. Pillai, T. K Das, Y. Singh and S. Maiti, Molecular effects of uptake of gold nanoparticles in HeLa cells. *Chem. Bio. Chem.* **8**, 1237–1240 (2007).
36. Y. Zhu, W. Li, Q. Li Y. Li, Y. Li, X. Zhang and Q. Huang, Effects of serum proteins on intracellular uptake and cytotoxicity of carbon nanoparticles. *Carbon* **47**, 1351–1358 (2009).
37. E. Brun, L. Sanche and C. Sicard-Roselli, Parameters governing gold nanoparticle X-ray radiosensitization of DNA in solution. *Colloids Surf. B* **72**, 128–134 (2008).
38. K. T. Butterworth, J. A. Wyer, M. Brennan-Fournet, C. J. Latimer, M. B. Shah, F. J. Currell and D. G. Hirst, Variation of strand break yield for plasmid DNA irradiated with high-Z metal nanoparticles. *Radiat. Res.* **170**, 381–387 (2008).
39. H. F. Dvorak, J. A. Nagy, J. T. Dvorak and A. M. Dvorak, Identification and characterization of the blood vessels of solid tumors that are leaky to circulating macromolecules. *Am. J. Pathol.* **133**, 95–109 (1988).
40. S. H. Cho, Estimation of tumour dose enhancement due to gold nanoparticles during typical radiation treatments: a preliminary Monte Carlo study. *Phys. Med. Biol.* **50**, N163–N173 (2005).
41. A. M. Kellerer and H. H. Rossi, RBE and the primary mechanism of radiation action. *Radiat. Res.* **47**, 15–34 (1971).
42. S. G. Sawant, R. Antonacci and T. Pandita, Determination of telomerase activity in HeLa cells after treatment with ionizing radiation by telomerase PCR ELISA. *Biochemica* **4**, 22–24 (1997).
43. E. J. Hall and J. L. Bedford, Dose rate: Its effects on the survival of HeLa cells irradiated with gamma rays. *Radiat. Res.* **22**, 305–315 (1964).
44. S. Kim, H-G. Wu, J. H. Shin, H. J. Park, I. A. Kim and H. Kim, Enhancement of radiation effects by flavopiridol in uterine cervix cancer cells. *Cancer Res. Treat.* **37**, 191–195 (2005).
45. B. Djordjevic and C. S. Lange, Cell-cell interactions in spheroids maintained in suspension. *Acta Oncol.* **45**, 412–420 (2006).
46. T. Helleday, E. Petermann, C. Lundin, B. Hodgson and R. A. Sharma, DNA repair pathways as targets for cancer therapy. *Nat. Rev. Cancer* **8**, 193–204 (2008).
47. N. Bhogal, F. Jalali and R. G. Bristow, Microscopic imaging of DNA repair foci in irradiated normal tissues. *Int. J. Radiat. Biol.* **85**, 732–746 (2009).
48. R. G. Bristow and R. P. Hill, Hypoxia and metabolism. Hypoxia, DNA repair and genetic instability. *Nat. Rev. Cancer* **8**, 180–192 (2008).
49. J. P. Banath and P. L. Olive, Expression of phosphorylated histone H2AX as a surrogate of cell killing by drugs that create DNA double-strand breaks. *Cancer Res.* **63**, 4347–4350 (2003).
50. S. J. McMahon, M. H. Mendenhall, S. Jain and F. Currell, Radiotherapy in the presence of contrast agents: a general figure of merit and its application to gold nanoparticles. *Phys. Med. Biol.* **53**, 5635–5651 (2008).
51. Y. Zheng and L. Sanche, Gold nanoparticles enhance DNA damage induced by anti-cancer drugs and radiation. *Radiat. Res.* **172**, 114–119 (2009).